



**Three-Dimensional Printed Horn Antennas with
Dielectric Lens for Free-Space Constitutive
Parameters Measurement**

by

**Renukka A/P Sivakumar
(2040813325)**

A dissertation submitted in fulfillment of the requirements for the degree of
Doctor of Philosophy

**Faculty of Electronic Engineering & Technology
UNIVERSITI MALAYSIA PERLIS**

2024

UNIVERSITI MALAYSIA PERLIS

ACKNOWLEDGEMENT

First and foremost, all praise, thank and gratitude to Jesus who bestowed His countless blessings upon me and provided me health and courage to complete this work.

This thesis is a conclusion of my whole Ph.D. study. I have to say that the acknowledgement is the most difficult part for me in this thesis, because there are too many people I wish to acknowledge. Without these people, I don't know how my life would be. Before anything, I would like to express my gratitude to my respectable supervisors Dr Saidatul Norlyana, Dr Soh Ping Jack, Dr You and Dr Lee who have been abundantly helpful during these years. Their continuous guidance, encouraging, valuable discussion and comments enhanced the work intensively and strengthen the scientific research value.

Dr Saidatul Norlyana Azemi has been the main supervisor for this thesis. Associate Prof. Dr. Ping Jack Soh, my co-supervisor, is deeply appreciated for taking this thesis in charge. The current thesis would have never seen the light of day without their support and encouragement. Words are insufficient in describing my sense of gratitude to them. Their suggestions and support during the period study are valuable, and it helped me a lot particularly in the difficult time.

Thanks then go to Dr Kok Yeow You, senior lecturer at Faculty of Electrical Engineering, Universiti Teknologi, Skudai, Johor, Malaysia for providing us the measurements facilities at UTM. Without him, it would be very hard for me to finish my work successfully on time.

Last but not least, this thesis is dedicated to my most beloved ones, the light of my life, my respected parents Sivakumar and Veni and my sibling Mineesha. In particular, I am sincerely grateful to my mother and father. In all my life I have been truly mesmerized by your devotion and true love. You have been a tremendous support in all my endeavors and always believed in me. This thesis would have never been possible without all of you.

TABLE OF CONTENTS

	PAGE
DECLARATION OF THESIS	ii
ACKNOWLEDGEMENT	iii
TABLE OF CONTENTS	iv
LIST OF TABLES	viii
LIST OF FIGURES	x
LIST OF ABBREVIATIONS	xvii
LIST OF SYMBOLS	xix
ABSTRAK	xxii
ABSTRACT	xxiii
CHAPTER 1 : INTRODUCTION	
1.1 Research Background	1
1.2 Problem statement	4
1.3 Research Objective	6
1.4 Research Scope	7
1.5 Research Contributions	8
1.6 Thesis Organization	10
CHAPTER 2 : LITERATURE REVIEW	
2.1 Introduction	12
2.2 Permittivity and Permeability	13
2.3 Techniques for dielectric properties measurement	14

2.3.1	Free Space	16
2.3.2	Open-ended coaxial probe method	17
2.3.2	Transmission Lines	20
2.3.4	Resonant Cavity method	21
2.4	Free space material measurement systems	21
2.5	Characterization of dielectric materials	23
2.6	Algorithms for calculation of material properties	30
2.6.1	NRW method	31
2.6.2	NIST Iterative method	38
2.6.2	New Non- Iterative method	41
2.6.4	Conversion algorithms	43
2.7	Calibration techniques	45
2.7.1	Thru-Reflect-Line (TRL) calibration	45
2.7.2	Thru-Reflect-Match (TRM) calibration	48
2.7.3	Types of calibration techniques	49
2.8	Horn antenna analysis	51
2.9	Commercial horn antenna	54
2.10	Lenses	56
2.10.1	Horn with lens analysis	60
2.10.2	Dielectric lens	65
2.11	Software used for material characterization	65
2.12	Sensitivity analysis	67
2.13	Far field and friss equation	69
2.14	Research gap	71
2.15	Summary	73
CHAPTER 3 : METHODOLOGY		
3.1	Introduction	74
3.2	Research flowchart	76

3.3	Modified NRW algorithm development	79
3.4	Design and development of horn antenna	83
3.4.1	3-D Printed K-band circular horn antenna	87
3.4.2	3-D Printed Ka-band circular horn antenna	90
3.5	Development and design of dielectric lens	92
3.6	Samples used for testing	99
3.7	Experimental setup for free space measurements	100
3.8	Summary	113
CHAPTER 4 : RESULTS & DISCUSSION		
4.1	Introduction	115
4.2	Parametric analysis result and discussion	115
4.2.1	Parametric analysis on K-band antenna	115
4.2.2	Parametric analysis on Ka-band antenna	121
4.2.3	Parametric analysis on distance between horn antenna and lens	125
4.3	Optimized Horn Antenna Dimension and Parameters	126
4.4	K-band and Ka-band horn antennas using 3D printing technology	127
4.4.1	Result and discussion of 3-D printed K-band horn antenna	127
4.4.2	Result and discussion of 3-D printed Ka-band horn antenna	130
4.5	Result and discussion of 3-D printed dielectric lens	134
4.5.1	3-D printed K-band horn antenna results with lens	138
4.5.2	3-D printed K-band horn antenna results with lens	142
4.5.3	Comparison of 3dB beamwidth for 3-D printed horn antennas and commercial horn antenna	145
4.5.4	Comparison of gain for 3-D printed K-band, Ka-band antenna and commercial horn antenna	147
4.6	Measured dielectric properties of MUT using modified NRW algorithm	149
4.7	Dielectric properties using Modified and Unmodified NRW	169
4.8	Mean absolute Percentage Error (MAPE)	177

4.9	Comparison in terms of antenna and lens	181
4.10	Comparison in terms of NRW algorithm	183
4.11	Summary	185

CHAPTER 5 : CONCLUSION

5.1	Recommendations for future work	189
-----	---------------------------------	-----

REFERENCES	191
-------------------	------------

LIST OF PUBLICATIONS	200
-----------------------------	------------

@This item is protected by original copyright

LIST OF TABLES

	PAGE	
Table 2.1	Comparison of Different Material Measurement Techniques	16
Table 2.2	Free Space Material Measurement Systems	22
Table 2.3	Measurement Techniques Advantages and Disadvantages	24
Table 2.4	Samples With Different Thickness and Loss Tangents	25
Table 2.5	Complex Permittivity Obtained using Transmission-Reflection Method	25
Table 2.6	Dielectric properties of PTFE and PMMA for different Distances between the Samples and ANTENNAS	27
Table 2.7	Dielectric Data for mouse liver for different measurement scenarios	28
Table 2.8	Material properties of different materials	29
Table 2.9	Material Permittivity of different substances	30
Table 2.10	Algorithms and calculations in measurement methods	31
Table 2.11	Conversion Algorithms	44
Table 2.12	Types of calibration	50
Table 2.13	Horn antenna analysis	52
Table 2.14	Commercial horn antenna electrical specifications	55
Table 2.15	Commercial horn antenna mechanical specifications	55

Table 2.16	State of the art of the lens structures	57
Table 2.17	Horn with lens analysis	61
Table 2.18	Types of software used	66
Table 3.1	K-band Horn Antenna Specifications	88
Table 3.2	Ka-band Horn Antenna Specifications	90
Table 3.3	Focal length and radius of curvature of K-band and Ka-band horn antenna	94
Table 4.1	K-band Horn Antenna Dimension	126
Table 4.2	K-band Horn Antenna Parameters	126
Table 4.3	Ka-band Horn Antenna Dimension	126
Table 4.4	Ka-band Horn Antenna Parameters	127
Table 4.5	MUTs dielectric constant at GHz frequency (Handoko et al.,2021; Vocke & Moser, 2022b; Wanget al., Roy et al.,2022)	151
Table 4.6	MUTs loss tangent at GHz frequency (Handako et al., 2021; Lee et al., 2019; Vocke & Moser, 2022).	151
Table 4.7	Comparison in terms of antenna and lens	182
Table 4.8	Comparison in terms of NRW algorithm	184

LIST OF FIGURES

	PAGE
Figure 1.1 Applications of dielectric properties	3
Figure 2.1 Electromagnetic field interaction and the relation between permittivity and permeability	14
Figure 2.2 Measurement ranges of various methods	15
Figure 2.3 Free space method	17
Figure 2.4 Coaxial probe technique	18
Figure 2.5 Transmission-Reflection method	20
Figure 2.6 Resonant method	21
Figure 2.7 Flow of NRW method	32
Figure 2.8 Measurement setup	33
Figure 2.9 Effective dielectric constants of cement	34
Figure 2.10 Representations of the different calculation algorithms for free space measurement systems	35
Figure 2.11 Flowchart of unambiguous retrieval of material properties	37
Figure 2.12 Flowchart of NIST ITERATIVE method algorithm	39
Figure 2.13 Flowchart of New Non-Iterative method algorithm	42
Figure 2.14 Free space TRL “REFLECT” step using metal plate	46
Figure 2.15 Free space TRL “THRU” step	46
Figure 2.16 “THRU” step	47

Figure 2.17	“REFLECT” step	47
Figure 2.18	“LINE” step	48
Figure 2.19	TRM calibration technique	49
Figure 2.20	Commercial horn antenna dimensions	54
Figure 2.21	Commercial horn antenna	54
Figure 2.22	Plano-convex lens	58
Figure 2.23	3-D printed lens	58
Figure 2.24	Electric field distribution	65
Figure 2.25	The proposed technique	69
Figure 2.26	Far field equations representations	70
Figure 2.27	Wavefront of far field and near field	70
Figure 2.28	Friss equation diagram	70
Figure 3.1	Research flowchart	78
Figure 3.2	Modified NRW algorithm flowchart	80
Figure 3.3	IIR Filtering Method	81
Figure 3.4	Unmodified NRW in MATLAB	81
Figure 3.5	Modified NRW in MATLAB	82
Figure 3.6	Block diagram for modified algorithm development	83
Figure 3.7	Pyramidal horn design equations representations	84
Figure 3.8	Conical horn design equations representations	85
Figure 3.9	Design of waveguide	86

Figure 3.10	Evolution of horn antenna	87
Figure 3.11	Dimensions of the proposed K-band antenna	88
Figure 3.12	Cutting plane of K-band horn antenna	89
Figure 3.13	Dimensions of the proposed Ka-band horn antenna	90
Figure 3.14	Lens antenna configuration	93
Figure 3.15	Representations of radius of curvature, thickness of lens and aperture radius	93
Figure 3.16	Dielectric lens antenna view for K-band antenna	95
Figure 3.17	Dielectric lens antenna view for Ka-band antenna	96
Figure 3.18	Dielectric lens front view, side view	97
Figure 3.19	Design of dielectric lens in CST	97
Figure 3.20	Design of dielectric lens in Creality Slicer	98
Figure 3.21	3-D Printing process	99
Figure 3.22	Front, back, side view of 3-D printed dielectric lens	99
Figure 3.23	Samples used for testing	100
Figure 3.24	Measurement set up without lens	101
Figure 3.25	Measurement set up with lens	101
Figure 3.26	Measurement set up with lens with 3-D printed horns	102
Figure 3.27	Dielectric properties measurement software interface	105
Figure 3.28	Open short load calibration in VNA	106
Figure 3.29	TRL classes and its calibration kit	107
Figure 3.30	TRL reflect step	108

Figure 3.31	TRL thru calibration	109
Figure 3.32	Measurement diagram with mechanical jigs	110
Figure 3.33	Farfield calculations diagram	110
Figure 3.34	“THRU” step	112
Figure 3.35	“Reflect” step	112
Figure 3.36	“Line” step	113
Figure 4.1	Parametric analysis on horn flare diameter for K-band horn antenna	117
Figure 4.2	Parametric analysis on coaxial probe inner diameter of K-band horn antenna	118
Figure 4.3	Parametric analysis on length of pin for K-band horn antenna	119
Figure 4.4	Parametric analysis on distance between horn antenna and lens	120
Figure 4.5	Parametric analysis on horn flare diameter for Ka-band horn antenna	121
Figure 4.6	Parametric analysis on coaxial probe inner diameter of K-band horn antenna	122
Figure 4.7	Parametric analysis on length of pin for Ka-band horn antenna	123
Figure 4.8	Parametric analysis on distance between horn antenna and lens	124
Figure 4.9	Diagram of distance between the horn antenna and lens	125
Figure 4.10	Diagram of spherical wave from horn antenna converting to plane wave	126

Figure 4.11	S_{11} simulation results and measurement results for K-band antenna	128
Figure 4.12	3-D radiation pattern for K-band antenna	129
Figure 4.13	Radiation pattern for K-band antenna in terms of E-plane and H-plane	130
Figure 4.14	S_{11} simulation results and measurement results for Ka-band antenna	131
Figure 4.15	3-D radiation pattern for Ka-band antenna	132
Figure 4.16	Radiation pattern for Ka-band antenna in terms of E-plane and H-plane	133
Figure 4.17	E-field distribution of the lens for the K-band antenna	135
Figure 4.18	Dielectric lens converting from spherical wave to plane wave	136
Figure 4.19	E-field distribution of the lens for Ka-band antenna	137
Figure 4.20	Measurement results for K-band antenna with and without lens	139
Figure 4.21	3-D radiation pattern of the K-band horn antenna with lens	140
Figure 4.22	Radiation pattern of the K-band horn antenna with and without lens on E-plane	141
Figure 4.23	Measurement results for Ka-band antenna with and without lens	143
Figure 4.24	3-D radiation pattern of the Ka-band horn antenna with lens	144
Figure 4.25	Radiation pattern of the Ka-band horn antenna with and without lens on E-plane	145
Figure 4.26	3-dB beamwidth of K-band antenna with and without lens	147

Figure 4.27	Gain of K-band, Ka-band and commercial horn antenna with and without lens	149
Figure 4.28	ϵ_r of FR4 with and without lens	153
Figure 4.29	μ_r of FR4 with and without lens	153
Figure 4.30	Loss tangent of FR4 with and without lens	154
Figure 4.31	ϵ_r of polypropylene with and without lens	155
Figure 4.32	μ_r of polypropylene with and without lens	155
Figure 4.33	Loss tangent of polypropylene with and without lens	156
Figure 4.34	ϵ_r of ABS with and without lens	157
Figure 4.35	μ_r of ABS with and without lens	157
Figure 4.36	Loss tangent of ABS with and without lens	158
Figure 4.37	ϵ_r of polycarbonate with and without lens	159
Figure 4.38	μ_r of polycarbonate with and without lens	159
Figure 4.39	Loss tangent of polycarbonate with and without lens	160
Figure 4.40	ϵ_r of PVC with and without lens	161
Figure 4.41	μ_r of PVC with and without lens	161
Figure 4.42	Loss tangent of PVC with and without lens	162
Figure 4.43	ϵ_r of acrylic with and without lens	163
Figure 4.44	μ_r of acrylic with and without lens	163
Figure 4.45	Loss tangent of acrylic with and without lens	164
Figure 4.46	ϵ_r of Teflon with and without lens	165
Figure 4.47	μ_r of Teflon with and without lens	165

Figure 4.48	Loss tangent of Teflon with and without lens	166
Figure 4.49	ϵ_r of epoxy with and without lens	167
Figure 4.50	μ_r of epoxy with and without lens	167
Figure 4.51	Loss tangent of epoxy with and without lens	168
Figure 4.52	Modified and Unmodified NRW permittivity and permeability of FR4	169
Figure 4.53	Modified and Unmodified NRW permittivity and permeability of polypropylene	170
Figure 4.54	Modified and Unmodified NRW permittivity and permeability of ABS	171
Figure 4.55	Modified and Unmodified NRW permittivity and permeability of polycarbonate	172
Figure 4.56	Modified and Unmodified NRW permittivity and permeability of PVC	173
Figure 4.57	Modified and Unmodified NRW permittivity and permeability of acrylic	174
Figure 4.58	Modified and Unmodified NRW permittivity and permeability of teflon	175
Figure 4.59	Modified and Unmodified NRW permittivity and permeability of epoxy	176
Figure 4.60	Mean absolute percentage error for permittivity of the MUTs	178
Figure 4.61	Mean absolute percentage error for permeability of the MUTs	179

LIST OF ABBREVIATIONS

THZ	Terahertz
VNA	Vector Network Analyzer
MMW	Millimeter-Wave
PCB	Printed Circuit Board
MUT	Material Under Test
TRL	Thru-Reflect-Line
NRW	Nicholson Ross Weir
TRM	Thru Reflect Match
LRL	Line-Reflect-Line
OSL	Open-Short-Load
PMMA	Polymethylmethacrylate
PTFE	Polytetrafluorethylene
PLA	Polylactic Acid
TFE	Time From Excision
TO	Transmission-Only
RO	Reflection-Only
TDG	Time Domain Gating
GRL	Gated Reflect Line
SNR	Signal-to-Noise Ratio
ABS	Acrylonitrile butadiene styrene
FDM	Fused Deposition Modelling
PC	Polycarbonate
PP	Polypropylene
PVC	Polyvinyl chloride
VSWR	Voltage Standing Wave Ratio
TDS	Time-Domain Spectroscopy

GCPW Grounded Coplanar Waveguide
FSM Free Space Method

@This item is protected by original copyright

LIST OF SYMBOLS

ϵ	Electric Permittivity
ϵ_0	Permittivity of vacuum
ϵ_r	Dielectric constant
μ	Magnetic permeability
μ_0	Permeability of free space
S_{11}, S_{21}	S-parameters
Γ	Reflection coefficient
X	Transmission coefficient
λ_0	Free space wavelength
λ_c	Cut-off wavelength
σ_t	Effective electrical conductivity
d_t	Sample thickness
Δ	Error analysis
ϵ_{rt}	Relative complex permittivity
τ_{meas}	Measured group delay
τ_{cal}	Calculated group delay
η	Intrinsic impedance of the slab
k	Phase constant
d	Thickness of slab
η''	Imaginary refractive index
J	Jacobian matrix
J^{-1}	Inverse Jacobian matrix
γ	Propagation constant
c	Speed of light
$F(\epsilon_r)$	Permittivity of NIST Iterative method
μ_{eff}	Effective permeability

ϵ_{eff}	Effective permittivity
r^2	Coordinates
T	Thickness of the lens
D	Diameter of the lens
f	Focal length of the lens
R_1, R_2	Radius of the curvature
w	Beam radius
E	Horn flare diameter
C	Antenna thickness
W	Horn flare length
H	Waveguide width
P	Waveguide height
D_s	Distance of pin
D_l	Distance between horn and the sample
R	Distance of the whole linear guide rail
a	Reactive near field
b	Width of the horn antenna
ω_{in}	Height of the horn antenna
T_e	Input beam waist radius
F_e	Edge taper
r_e	Power of the gaussian beam
d_1	Radius of the gaussian beam
P_t	Power of transmitting antenna
P_r	Power of receiving antenna
G_t	Gain of transmitting antenna
G_r	Gain of receiving antenna

d

Distance from the MUT

@This item is protected by original copyright

Antena Tanduk Cetak Tiga Dimensi dengan Lensa Dielektrik untuk Pengukuran Parameter Konstitutif Ruang Bebas

ABSTRAK

Sepanjang dua dekad terakhir, terdapat perkembangan yang signifikan dalam teknologi gelombang mm dan terahertz (THz), didorong oleh sifat-sifat menarik mereka dalam pelbagai aplikasi, termasuk bahan cat automotif, struktur metamaterial, astronomi radio, tentera, dan bidang perubatan. Sebagai hasil daripada peningkatan permintaan untuk komponen dan sistem gelombang mm, terdapat keperluan yang lebih besar untuk penyelesaian pengukuran yang berkesan kos dalam julat frekuensi ini dan di luar. Teknik pengukuran ruang bebas adalah kaedah yang digunakan secara meluas untuk menentukan ciri-ciri elektrik bahan. Penyelidikan doktorat ini bertujuan untuk memberi tumpuan kepada pembangunan sistem pengukuran bahan ruang bebas yang mampu menentukan dengan tepat permeabiliti dan permedian bahan. Sebuah program perisian melalui algoritma NRW yang diubahsuai yang boleh menentukan permeabiliti bahan dan permedian dengan ketepatan yang tinggi telah dibangunkan daripada perisian komersial yang mahal. Juga, permeabiliti dan permedian MUT telah ditentukan dengan ketepatan yang tinggi melalui perisian dengan dan tanpa lensa untuk antena tanduk komersial dan 3D cetak tanduk antena. Antena K-band dan Ka-band dari 18 GHz hingga 39 GHz menggunakan teknologi percetakan 3D telah direka untuk mengatasi keperluan sistem pengukuran komersial yang mahal. Untuk mengurangkan ketidaktepatan pengukuran, lensa dielektrik dicetak 3D telah direka dan dihasilkan melalui teknologi pencetakan 3D di mana fokus sinar antena dioptimumkan. Antena tanduk dicetak 3D menunjukkan kesepakatan yang baik dengan antena tandukan komersial dalam hal S11, VSWR, keuntungan dan lebar sinar 3-dB. Mengenai keuntungan, dengan penggunaan lensa, keuntungan meningkat dengan keuntungan maksimum 25.7 dBi pada 26 GHz apabila dibandingkan dengan keuntungan tanpa penggunaan objektif dengan faedah maksimum 15.6 dBi di 26GHz untuk antena tanduk K-band. Juga, untuk keuntungan, dengan penggunaan lensa, keuntungan meningkat dengan keuntungan maksimum 26.5 dBi pada 32 GHz apabila berbanding dengan keuntungan tanpa penggunaan objektif dengan faedah maksimum 15.5 dBi pada 32GHz untuk antena tanduk Ka-band. Tanpa penggunaan lensa, lebar sinar 3-dB berada dalam julat 33o hingga 41.5o manakala dengan penggunaan objektif, lebarnya 3 dB berada di julat 8.9o hingga 9.7o untuk antena tanduk K-band. Penggunaan lensa membolehkan lebar beam yang sempit yang memberi tumpuan isyarat dalam arah tertentu di seluruh julat frekuensi K-band. Mengenai antena tanduk Ka-band tanpa penggunaan lensa, lebar sinar 3-dB berada dalam julat 28o hingga 50o manakala dengan penggunaan objektif, lebarnya sinar 3 dB berada di julat 7o hingga 9o. Mengenai pengedaran medan E untuk lensa dielektrik, ia meningkat kerana frekuensi meningkat yang ialah dari 549 V / m pada 18 GHz kepada 855 V / M pada 26 GHz untuk antena tanduk K-band. Mengenai antena tanduk Ka-band, pengedaran medan E untuk lensa dielektrik meningkat daripada 855 V/m pada 26 GHz kepada 941 V / m pada 39 GHz

Three-Dimensional Printed Horn Antennas with Dielectric Lens for Free-Space Constitutive Parameters Measurement

ABSTRACT

Over the last two decades, there has been significant development in mm-wave and terahertz (THz) technologies, driven by their appealing properties in various applications, including automotive paint materials, metamaterial structures, radio astronomy, military, and medical field. Additionally, the use of dielectric properties for material identification has proven valuable in mm-wave imaging systems. As a result of the increased demand for mm-wave components and systems, there is a greater need for cost-effective measurement solutions in this frequency range and beyond. The free-space measurement technique is widely used methods for determining the electrical characteristics of materials. This doctoral research aims to focus on the development of a free space material measurement system capable of accurately determining materials' permeability and permittivity. A software program through modified NRW algorithm which could determine the materials' permeability and permittivity with high accuracy was developed rather than expensive commercial software. Also, the permeability and permittivity of MUTs were determined with high accuracy through the software with and without lens for the commercial horn antenna and 3-D printed horn antennas. High gain K-band and Ka-band horn antennas from 18 GHz to 39 GHz using 3D printing technology were designed in order to overcome the need for costly commercial measurement systems. To mitigate the measurement inaccuracies, 3-D printed dielectric lens was designed and fabricated through 3-D printing technology in which beam focus of antenna optimized. 3-D printed horn antennas showed a good agreement with the commercial horn antenna in terms of S_{11} , VSWR, gain and 3- dB beamwidth. As for the gain, with the use of lens the gain increased with a maximum gain of 25.7 dBi at 26 GHz when compared to the gain without the use of lens with a maximum gain of 15.6 dBi at 26 GHz for the K-band horn antenna. Also, for the gain, with the use of lens the gain increased with a maximum gain of 26.5 dBi at 32 GHz when compared to the gain without the use of lens with a maximum gain of 15.5 dBi at 32 GHz for the Ka-band horn antenna. Without the use of lens, 3- dB beamwidth is in the range of 33° to 41.5° while with the use of lens, the 3- dB beamwidth is in the range of 8.9° to 9.7° for the K-band horn antenna. Use of lens allows narrowed beamwidth which focus signals in particular direction throughout the K-band frequency range. As for the Ka-band horn antenna without the use of lens, 3- dB beamwidth is in the range of 28° to 50° while with the use of lens, the 3- dB beamwidth is in the range of 7° to 9° . As for the E-field distribution for the dielectric lens, it increased as the frequency increased which is from 549 V/m at 18 GHz to 855 V/m at 26 GHz for the K-band horn antenna. As for the Ka-band horn antenna, the E-field distribution for the dielectric lens increased from 855 V/m at 26 GHz to 941 V/m at 39 GHz.

CHAPTER 1: INTRODUCTION

1.1 Research Background

The characterization of dielectric materials plays a crucial role in understanding their properties. Having knowledge about dielectric properties in our everyday lives helps us comprehend how foods behave during microwave heating, how liquids function as dielectrics in transformers, and how they serve as insulating layers in Printed Circuit Board (PCB) build-up. These examples highlight the significance of dielectric properties in our daily experiences. In the last twenty years, there has been a significant and intensive development of millimeter wave (mm-wave) and terahertz (THz) technologies. These advancements are attributed to their appealing properties, which find practical applications in various fields, including radio astronomy, military applications, and medical technologies.

The increasing demands for mm-wave components and systems created a renewed need for cost-effective test and measurement solutions within this band and beyond. One of the important steps in designing devices operating at these frequencies is to first determine the electrical properties of materials. These values affect the method to design various radio components, as their behaviour varies according to frequency. This need arises as most materials are typically characterized up to the microwave bands. Besides that, material characterization can also be applied to determine quality of agricultural and industrial products, and biomedical applications (Lim et al., 2018).

Various measurement techniques have been established to determine material characteristics, specifically dielectric properties in terms of permittivity and permeability at microwave frequencies. These techniques include the free space method, transmission line method, waveguide method, impedance, coaxial probe, and cavity methods (Brinker et al., 2020; Krupka, 2021; Ozturk & Tahir Güneşer, 2019; Sato et al., 2021; Y. Wang et al., 2020).

Amongst these techniques, the free space measurement technique is popular as it allows the measurement of reflection and transmission measurements without any physical contact with the sample (Sivakumar et al., 2022). This method is particularly well-suited for thin, flat-faced materials or other substances that can be shaped accordingly. With the increasing demand for efficient, accurate, and broadband material measurement systems utilizing higher mm-wave and THz frequencies.

In its most conventional form, a free space measurement set up comprises of a vector network analyser, two horn antennas, sample holder and measurement software. Each horn antenna will be placed as the transmitter and receiver antenna respectively, and the material under test (MUT) will be placed between them (Ozturk et al., 2017; Semenenko et al., 2019). To facilitate the process, a software can be integrated into the system to calibrate and automate free space measurements prior to calculating electromagnetic properties of materials. The increasing portability of measurement equipment such as VNAs and the wider application and increasing importance of mm-wave/THz material spectroscopy is foreseen to increase research and commercial interest for this technique.

The renewed interest in the free-space measurement method stems from the increasing demand for new applications that necessitate efficient, accurate, and broadband material measurement systems operating at higher mm-wave and THz frequencies. Among the different types of measurement techniques, free space is preferred as it can use for high frequency measurements. Figure 1.1 shows the applications of dielectric properties. One of it, is determining the behaviour of foods during microwave heating. Also, liquid dielectric in transformers and insulating layer in the PCB build up are other applications of dielectric in our daily life.

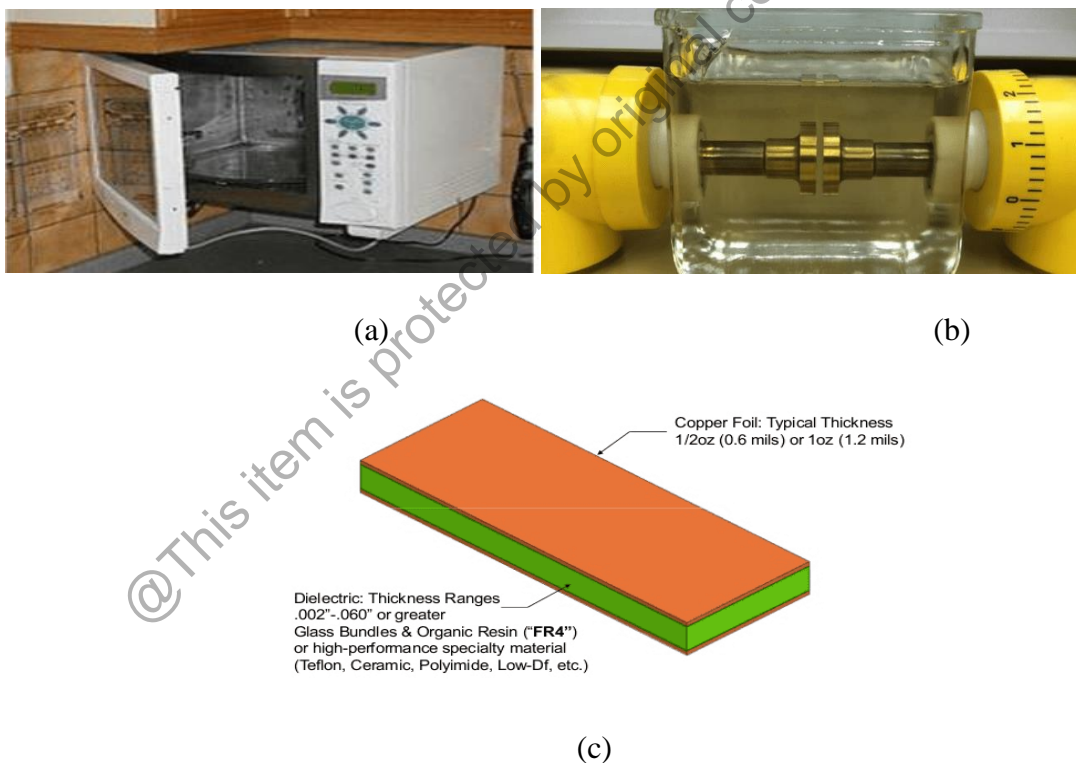


Figure 1.1 Applications of dielectric properties. (a) Microwave heating (Michalak et al., 2020) (b) Liquid dielectric in transformer (Tlhabologo et al., 2021) (c) As an insulating layer in PCB build up (Introduction to 3 Layer Printed Circuit Board (PCB), 2022)

At higher frequencies and beyond, applying the free space technique encounters challenges due to antenna beam growth, resulting in less energy concentrated on the dielectric slab (Alqahtani et al., 2022). To mitigate inaccuracies in measurements, a dielectric lens can be utilized to refocus the beam (Vohra et al., 2020). Nevertheless, the Through-Reflect-Line calibration is effective in reducing most errors (Vohra et al., 2020).

1.2 Problem statement

Current methods for producing K-band and Ka-band horn antennas, which operate in the 18 GHz to 39 GHz frequency range, often involve conventional manufacturing techniques that can be costly, time-consuming, and limited in terms of design flexibility (Jandyal et al., 2022; KUMAR, 2022; Yu-Lei et al., 2023).. These traditional fabrication methods may not efficiently support the intricate designs required for high gain antennas in these frequency bands. Moreover, the need for high precision in antenna geometry to achieve optimal performance at such high frequencies presents significant challenges. There is a growing demand for a more efficient, cost-effective, and versatile approach to antenna fabrication that can maintain, or even enhance, the performance characteristics required for applications in these higher frequency bands (Haghirosadat & Neshati, 2022; Shrestha et al., 2021; Tripathi et al., 2023). This project aims to address these challenges by exploring the potential of 3D printing technology for the design and fabrication of high gain K-band and Ka-band horn antennas, offering a novel solution that could revolutionize antenna manufacturing for high-frequency applications. (Jandyal et al., 2022).

The accuracy of free space measurements is often compromised by limitations in beam focusing and steering capabilities of horn antennas (Helmy et al., 2023; Khan et al., 2021; Piroutiniya et al., 2023). Horn antennas typically exhibit a finite beam width, which determines the angular range over which the antenna can effectively transmit or receive signals. Inaccuracies arise when the beam width is too wide, leading to signal spillage beyond the intended target area, or too narrow, resulting in incomplete coverage of the desired region. To address this challenge, this study aims to develop an innovative 3-D printed dielectric lens tailored specifically to optimize beam focusing and steering in horn antennas for free space measurements. Optimizing the beam focusing and steering capabilities of horn antennas through the development of a 3-D printed dielectric lens directly addresses the accuracy of free space measurements. By precisely controlling the propagation of electromagnetic waves, the dielectric lens enhances the antenna's ability to capture and transmit signals with minimal distortion or interference. (Helmy et al., 2023; Khan et al., 2021; Piroutiniya et al., 2023).

Some material measurement techniques and algorithms have inherent limitations, as they may not be capable of determining both permeability and permittivity of a material across various microwave frequency bands (L-band, S-band, C-band, X-band, Ku-band, K-band, Ka-band) and may be restricted to specific measurement frequencies (Ozturk & Tahir Güneşer, 2019). Apart from that, one of the issues that Nicholson Ross Weir (NRW) method suffers is the phase ambiguity which is caused by the branching problem of the algorithm (Hajisaeid et al., 2018; J. Y. Wang et al., 2017). This occurs when $-\infty \leq m \leq \infty$, where the results obtained are accurate up to the value of $m = 0$. Beyond that, the phase ambiguities will increase especially for thicker materials. In order to address this, the NRW approach has been altered to provide higher measurement

precision, particularly for more accurately nanostructured materials (Sharma & Dubey, 2022; Vakil et al., 2018). In addition, the resolution of the branching problem in the NRW technique was discussed in Singh et al. (2018). A different study in Singh et al. (2018) suggested an extraction technique for permittivity and permeability that could be used with any thickness of material. To overcome this, the NRW method has been modified for improved measurement accuracy for determination of dielectric properties of materials.

1.3 Research Objective

This research comprises of studies on horn antennas, dielectric lens, and determination of dielectric properties through free space material measurement system. The objectives of this thesis are as follows:

- i To design and fabricate high gain K-band and Ka-band horn antennas using 3D printing technology operating from 18 GHz to 39 GHz.
- ii To mitigate measurement inaccuracies by developing a 3-D printed dielectric lens that optimizes beam focusing and steering capabilities of the horn antenna.
- iii To develop a software program that utilizes the modified Nicolson Ross Weir (NRW) algorithm to accurately determine the permeability and permittivity of materials with high precision using mean absolute percentage error (MAPE).

1.4 Research scope

This dissertation primarily focuses on the development of a free space material measurement system capable of accurately determining materials' permeability and permittivity. The first phase involves the design of K-band and Ka-band horn antennas and a dielectric lens using the CST Studio Suite. Simulation results are then compared with those obtained from commercial horn antennas. Additionally, a dielectric lens is designed to ensure precise beam focus on the Material Under Test (MUT). Subsequently, the antennas, focusing mechanism, and mechanical jigs (such as sample holders and linear rails) are fabricated, leading to the creation of the free space setup. This setup comprises 3-D printed horn antennas, commercial horn antennas, the MUT, and the dielectric lens. The pyramidal horn antenna serves as the foundation for the evolution of horn antennas. The prior pyramidal horn antenna design did not produce the expected s-parameter results. This results in the circular horn antenna design. The cylinder shape was designed after the waveguide was designed using the frequency range. The final design was a circular horn antenna with a coaxial component.

In the next phase, the complete system, consisting of the antennas, focusing mechanism, and MUT, is simulated using appropriate software. Afterward, the optimized components and mechanical jigs are physically integrated, and the setup is subjected to testing. Utilizing a Vector Network Analyzer (VNA) for the measurement process, s-parameters are obtained. These parameters are then converted into materials' properties successfully through a simple software program, enabling the determination of the MUT s' permeability and permittivity.

Finally, the performance of the developed 3-D dielectric lens within the free space material measurement system will be thoroughly analysed and evaluated.

1.5 Research Contributions

There are research contributions of this dissertation. One of the contributions is designing and fabricating high gain K-band and Ka-band horn antennas using 3D printing technology. These antennas will be integrated into the free space measurement system in the frequency range from 18 GHz to 39 GHz. Paper published in AIP Publishing - *Sivakumar, Renukka, Lee Yeng Seng, Saidatul Norlyana Azemi, and Ping Jack Soh. "Mini double ridge horn antenna for free space measurement." In AIP Conference Proceedings, vol. 2579, no. 1. AIP Publishing, 2023 (Sivakumar et al., 2023)*. The final design was a circular horn antenna with a coaxial component. The prior pyramidal horn antenna design did not produce the expected s-parameter results. This results in the circular horn antenna design.

The second contribution of this dissertation is a designing and fabricating 3-D printed dielectric lens that optimizes beam focusing on the free space material measurement system. The dielectric lens will be placed in the free space material measurement system for concentration of the beam in determining the materials' permeability and permittivity accurately. Paper presented in ISAP 2023 - *Sivakumar, Renukka, Saidatul Norlyana Azemi, Azremi Abdullah Al-Hadi, ZahariAwang Ahmad, Kok Yeow You, Lee Yeng Seng, and Ping Jack Soh. "Horn Antenna Gain Enhancement using 3-D Printed Dielectric Lens for Dielectric Properties Measurement." In 2023 IEEE International Symposium on Antennas And Propagation (ISAP), pp. 1-2. IEEE, 2023 (Sivakumar et al., 2023)*.

The third contribution of this thesis is to develop a software program that utilizes modified NRW algorithm to determine materials' permeability and permittivity with high accuracy as published in our research paper (Sivakumar et al., 2022). The research was done using modified NRW algorithm on different samples to determine their permeability and permittivity. Filtering function was employed to smooth the permittivity and permeability plots. The method of infinite impulse response (IIR) filtering was applied to a signal in order to remove unwanted high frequency interference. The NRW code was modified with the filtering function in MATLAB. The modified code for the NRW in MATLAB was then integrated into the software and a dongle will be connected to the laptop to access the software. The software could be accessed after connecting to the laptop. The graphs of permeability and permittivity of the MUTs could be obtained from the software. 2 Paper was presented. 1 has been published in IEEE Proceeding and another one is scheduled to be publish – 1) Sivakumar, Renukka, Yeng Seng Lee, Saidatul Norlyana Azemi, Zahari Awang Ahmad, Ping Jack Soh, and Kok Yeow You. "A Free-Space Measurement System for Microwave Materials at Kuband." In 2022 IEEE International RF and Microwave Conference (RFM), pp. 1-4. IEEE, 2022 (Sivakumar et al., 2022). 2) Sivakumar, Renukka, Yeng Seng Lee, Saidatul Norlyana Azemi, Zahari Awang Ahmad, Ping Jack Soh, and Kok Yeow You., "Narrative Review on Advances in Measurement of Electrical Properties of Materials using Free Space Method" accepted and schedule to be published in Journal of Advanced Research in Applied Sciences and Engineering Technology.

1.6 Thesis Organization

This project report is can be allocated to 5 chapters which are introduction, literature review, methodology, results & discussion and conclusion.

Chapter 1 presents the introduction, problem statement, research question, objective, contribution, research framework and summary. The explanations about reconfigurable antenna also were included in this chapter.

Chapter 2 discusses about the literature review on different measurement techniques for material characterization, algorithms for determination of dielectric properties, calibration techniques and use of lens in material measurement. The measurement techniques which are free space method, resonant cavity method, transmission line method and coaxial method are explained in this chapter. Also, algorithms such as NRW method, NIST iterative method and New Non-Iterative method are illustrated here. Besides, calibration techniques such as (Thru-Reflect-Match) TRM calibration and (Thru-Reflect-Line) TRL calibration are discussed here. The application of lens in free space material measurement system are presented here.

Chapter 3 presents the description about the research methodologies which includes the design and specifications of K-band horn antenna, Ka-band horn antenna and commercial horn antenna. Also, the design and fabrication of dielectric lens are presented here. The measurement set up, samples used for testing, mechanical jigs used and software used for determination of material's permeability and permittivity are discussed here. The calculations for far field distance, TRL calibration and lens are

included in this chapter.

Chapter 4 provides the details about the simulation and measurement results of K-band horn antenna, Ka-band horn antenna and commercial horn antenna. The comparison of 3-D printed horn antennas with the commercial horn antenna are done. The software results of MUTs permeability and permittivity are presented also. The comparison of results with and without dielectric lens also discussed in this chapter.

Finally in Chapter 5, the conclusion and future work for this dissertation are discussed.

@This item is protected by original copyright

CHAPTER 2: LITERATURE REVIEW

2.1 Introduction

The understanding of electrical parameters such as ϵ' and ϵ'' is crucial for any microwave applications. The determination of dielectric properties of materials has gained attention especially in the research fields such as biological research, material science, etc (Jiang et al., 2020; Kanahna & Keowsawat, 2023; Sun et al., 2023). Dielectric measurement is crucial because it can determine the electrical or magnetic characteristics of the materials. This chapter reviews on the measurement techniques available in characterizing the material properties, measurement procedures, conversion methods, calibration techniques and types of lenses from the past studies.

Electromagnetic characterization of materials can be divided into resonant or non-resonant methods. Resonant methods are used to determine material properties at some discrete frequencies or single frequency while non-resonant methods are used to obtain the material properties over a frequency range. Resonant methods are perturbation method with TM cavity geometry while non-resonant methods are free space measurement technique, open-ended coaxial probe method and transmission/reflection line method. Both these methods have been established to measure the permittivity and permeability of materials (Lu et al., 2022; Malkin et al., 2021; Nakamura et al., 2020). One of these techniques, is the free space measurement technique which is popular as it allows the measurement of transmission and reflection measurements without any physical interaction with the sample.

Some conversion methods are applied for determining the permittivity and permeability from s-parameters through vector network analyser. The conversion techniques are NRW, NIST iterative, and new non-iterative (Angiulli & Versaci, 2021; Ozturk & Tahir Güneşer, 2019). Calibrations need to be done before carrying out the measurement procedure for the material measurement system. There are several calibration methods available which are through-reflect-line (TRL), through-reflect-match (TRM) and line-reflect-line (LRL) (Guo et al., 2019; Koo et al., 2022; Ramezani et al., 2021). The calibration methods, algorithms, and calculations of dielectric properties, methods to improve measurement accuracy is discussed in this chapter. Besides, suitable parameter extraction algorithms are crucial. These two factors mainly determine the speed and accuracy of extraction in different measurement techniques. All these issues are reviewed in this section.

2.2 Permittivity and Permeability

Electric permittivity, ϵ , which represents the energy stored in an electric field, is the ratio of permittivity of the material ϵ_r to the permittivity of vacuum, ϵ_0 as in (Vohra et al., 2020). It also indicates the interaction of a material with electric fields, which is also indicated as the dielectric constant, in Equation (2.1). The real part of permittivity ϵ_r' is a count of the energy stored in a material. The imaginary part of permittivity, ϵ_r'' is the loss factor and determines how lossy a material is in the existence of an external electric field. Magnetic permeability, μ in Equation (2.2) is the energy stored in a magnetic field and μ_0 is the permeability of free space. Figure 2.1 shows the electromagnetic field interaction and the relation between permittivity and permeability (Vohra et al., 2020).

$$\epsilon_r = \frac{\epsilon}{\epsilon_0} \quad (2.1)$$

$$\mu_r = \frac{\mu}{\mu_0} \quad (2.2)$$

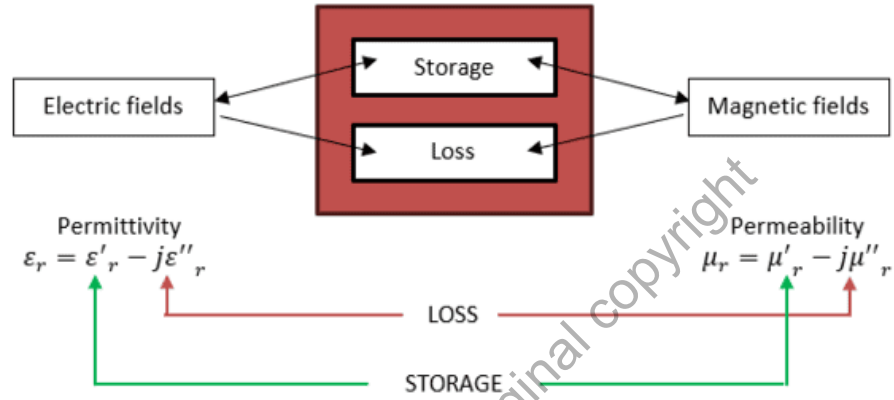


Figure 2.1 Electromagnetic field interaction and the relation between permittivity and permeability (Vohra et al., 2020).

2.3 Techniques for Dielectric Properties Measurement

This section will briefly present the available material property measurement techniques and compare them in terms of their suitability for different applications as in A summary of the well-known material measurement techniques is presented in Figure 2.2. Each measurement technique operates in different frequency ranges as each one of them limited to specific frequencies, materials, applications. The free-space measurement technique is mostly applicable for a wide range of frequencies from 5 GHz to 330 GHz. On the other hand, the transmission line measurement technique is applicable from 50 MHz to 60 GHz, whereas the coaxial probe measurement capability ranges from 50 MHz to 40 GHz. The resonant cavity method is typically used to measure materials from 5

GHz to 20 GHz. On the contrary, the parallel plate measurement technique is only applicable at frequencies up to only 50 MHz. Coaxial probe and transmission line methods exhibit rather high losses and is moderate for the parallel plate and free space techniques are moderate. The measurement technique which features the relatively lowest loss is the resonant cavity method.

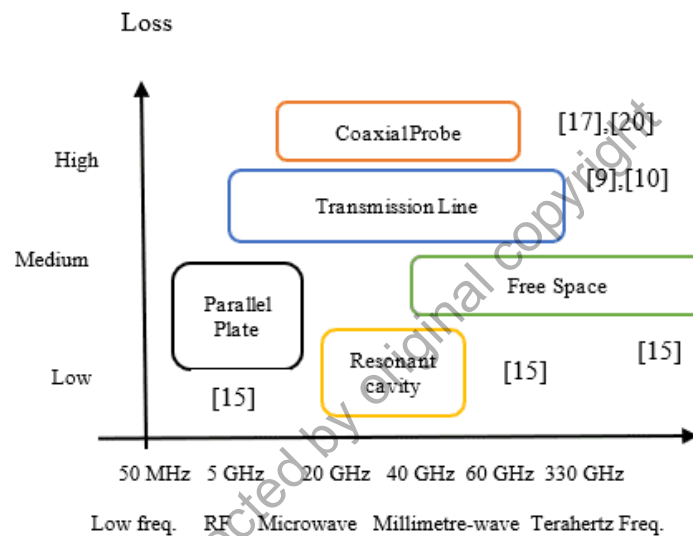


Figure 2.2 Measurement ranges of various methods (Sivakumar et al., 2023)

Table 2.1 presents the state of the art of material measurement techniques in terms of operating frequencies, types of dielectric properties measured using each technique, types of suitable materials for measurements, level of losses, and measurement conversion techniques. The free space measurement technique can measure material permittivity and permeability by extraction and calculation of S -parameters for a wide range of frequencies. The transmission line method has similar capabilities except for the difference is its measurement frequency range. The coaxial probe and parallel plate methods, on the other hand, can extract S_{11} and thus can only retrieve ϵ_r . Finally, the

resonant cavity method determines both the permittivity and permeability of a material, and unlike the other measurement techniques, it extracts the quality factor Q -factor and the resonant frequencies of microwave resonators from their S -parameters.

Table 2.1 Comparison of Different Material Measurement Techniques (Sivakumar et al., 2023)

Measurement techniques	Coaxial probe	Transmission line	Free space	Resonant cavity
Operating frequency	50 MHz-50 GHz	50 MHz-60 GHz	5 GHz-330 GHz	5 GHz-20 GHz
Dielectric properties	ϵ_r	ϵ_r, μ_r	ϵ_r, μ_r	ϵ_r, μ_r
S-parameters	S11	S11, S21	S11, S21	Q-factors
Materials	Biological specimens, liquids	Waveguide	Large solids, liquids	Solid materials, liquids, waveguides
Loss	High	Medium	Medium	Low
Conversion techniques	RFM	NRW, NIST iterative	NRW, NIST iterative	Frequency & Q-factors

2.3.1 Free Space

A free-space measurement setup consists of a vector network analyser (VNA), horn antennas, sample holder and measurement software. Both horn antennas will be used as the receiver and transmitter and the material under test (MUT) will be positioned between them as in (Vohra & El-Shenawee, 2021; Cai et al., 2022; Jung et al., 2019). The software automates the relative complex permittivity, ϵ_r and relative complex

permeability, μ_r measurements through S -parameters obtained through the VNA. For example, a commercial materials measurement software from Keysight Technologies streamlines the process of measuring ϵ_r and μ_r using a VNA, with its setup shown in Figure 2.3 (Vohra & El-Shenawee, 2021). It is applicable in determining dielectric properties of materials in applications, such as agriculture, biomedical, and material engineering.

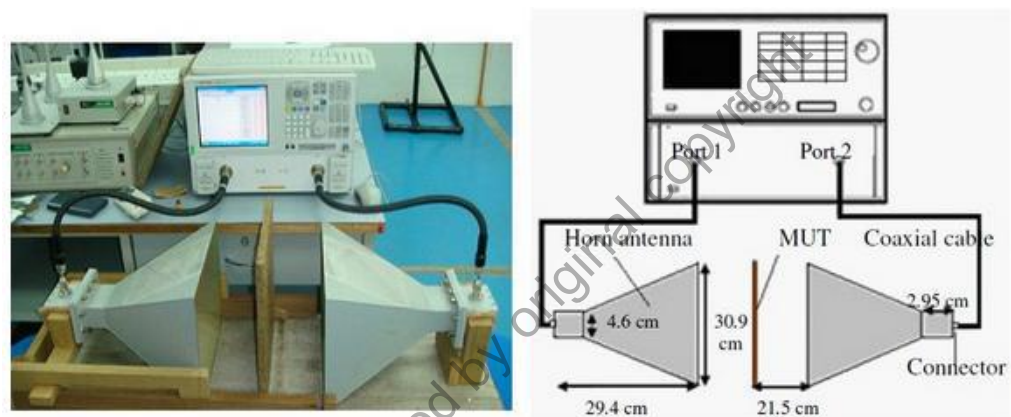


Figure 2.3 Free space method (Vohra & El-Shenawee, 2021)

2.3.2 Open ended coaxial probe method

This method uses a coaxial probe which probe aperture is placed into the liquids or semi-solids to determine their permittivity as shown in Figure 2.4 (La Gioia et al., 2018). VNA is used to determine the reflection coefficient, Γ then convert the measured Γ into relative complex permittivity, ϵ_r . The coaxial probe calibration process involves the open-circuit, short-circuit, and broadband load standards, namely open-short-load (OSL) calibration method. This technique can also be used for dielectric measurement of biological tissues (La Gioia et al., 2018). Figure 4 shows the schematic of the measurement setup for open-ended coaxial probe method which involves the use of the

VNA for the determination of dielectric properties from 50 MHz to 50 GHz. The sample preparation is easy for this method as it need no machining of the sample. During measurement, the method may be affected by air gaps.

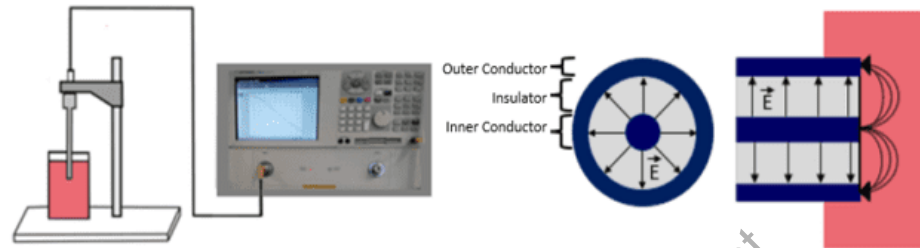


Figure 2.4 Coaxial probe technique (La Gioia et al., 2018)

2.3.3 Transmission Lines

In this method, a sample is placed in a portion of coaxial line and the measurement done using a VNA from 50 MHz to 60 GHz. The VNA is first calibrated prior to measurements, and the obtained S -parameters are converted to dielectric properties using conversion methods such as NRW method or NIST iterative methods. Equations (2.3) to (2.9) was solved through an external or internal software program for NRW method as in (Ziyao et al., 2023). The measurement setup is shown in Figure 2.5 (Ziyao et al., 2023). One of the advantages of this method is, it is able to determine both the permeability and permittivity of the samples. Effects of air gap during measurement is the limitation of this method.

The S -parameters acquired from the functions of the VNA can be computed using Equations (2.3) and (2.4), as follows:

$$S_{11} = \frac{\Gamma(1-T^2)}{1-\Gamma^2T^2} \quad (2.3)$$

and

$$S_{21} = \frac{T(1-\Gamma^2)}{1-\Gamma^2T^2} \quad (2.4)$$

The reflection coefficient, Γ can then be procured through Equation (2.5) and Equation (2.6), where X used to find the correct roots for the condition of $|\Gamma| < 1$.

$$\Gamma = X \pm \sqrt{X^2 - 1} \quad (2.5)$$

The transmission coefficient, T is shown in Equation (2.7) while the relative complex permeability, μ_r is shown in Equation (2.8) as:

$$X = \frac{S_{11}^2 - S_{21}^2 + 1}{2S_{11}} \quad (2.6)$$

and

$$T = \frac{S_{11} + S_{21} - \Gamma}{1 - (S_{11} + S_{21}\Gamma)} \quad (2.7)$$

$$\mu_r = \frac{1 + \Gamma}{A(1 - \Gamma) \left[\sqrt{\frac{1}{\lambda_o^2 - \lambda_c^2}} \right]} \quad (2.8)$$

$$\frac{1}{A^2} = - \left[\frac{1}{2\pi L} \ln \left(\frac{1}{T} \right) \right]^2 \quad (2.9)$$

Finally, the relative complex permittivity, ϵ_r of the material can be determined using Equation (2.10).

$$\epsilon_r = \frac{\lambda_0^2}{\frac{\mu_r}{\lambda_c^2} \left[\frac{1}{2\pi L} \ln\left(\frac{1}{T}\right) \right]^2} \quad (2.10)$$

where λ_0 is the free space wavelength while λ_c represents the cut-off wavelength. Equations (2.9) and (2.10) have an endless number of roots because the term's imaginary part $\ln(1/T)$ is equal to $j(\Theta + 2\pi n)$ where $n=0, \pm 1, \pm 2, \dots$, the integer of (L/λ_g) .

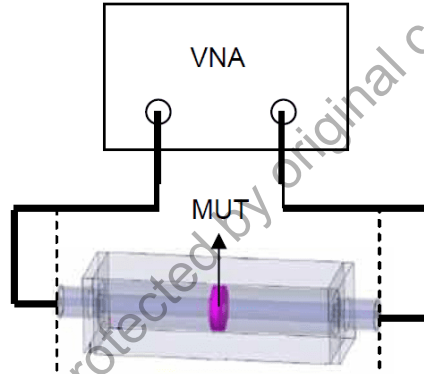


Figure 2.5 Transmission-Reflection method (Ziyao et al., 2023)

2.3.4 Resonant Cavity Method

Resonant cavity method is method used to determine material properties of liquids, waveguides and rod-shaped solid materials using cavities which resonates at specific frequencies. Despite its limitation to a single frequency which is a specific frequency, it features improved measurement accuracy. When material samples are placed in the cavity, changes in the field interaction will cause shift in the measured resonance and Q -factor which results in determination of the sample properties. Figure 2.6 presents the schematic representation of resonant cavity method as in (Li et al., 2023).

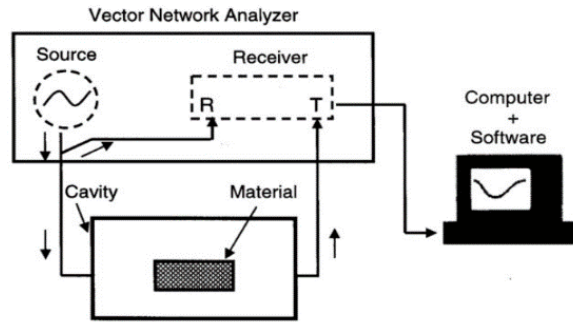
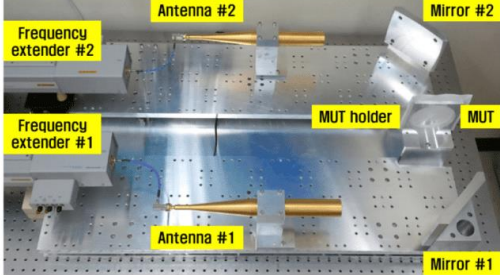
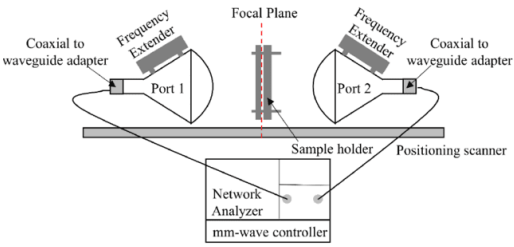
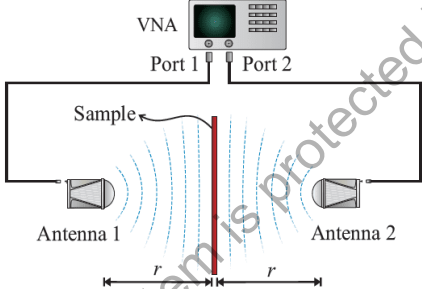
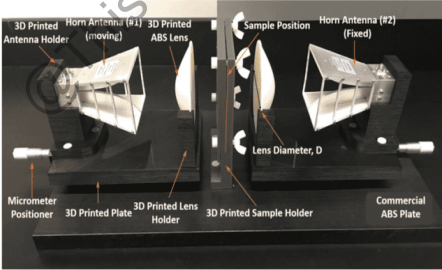


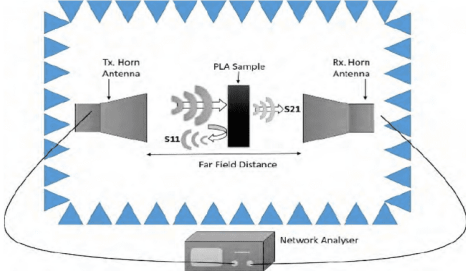
Figure 2.6 Resonant method (Li et al., 2023)

2.4 Free space material measurement systems

Free space methods were carried out in different frequency ranges, different types of samples as tabulated in Table 2.2. The free space measurement setup varies in terms of usage of frequency extenders, types of MUT's used in certain frequency ranges. One of the researchers focused on free space measurement from 75 GHz to 110 GHz for the samples such as air and plastic plate (Kang & Kim, 2019). (Vohra & El-Shenawee, 2021) tested the radar absorbing materials for the extraction of permittivity. (Gonçalves et al., 2018) focused on samples such as Polymethylmethacrylate (PMMA) and Polytetrafluorethylene (PTFE) while (Malik et al., 2019) tested Polylactic Acid sample. (Hajisaeid et al., 2018) tested more samples compared to other studies as in Table 2.2, which are polyimide film, liquid crystalline polymer sheet, polypropylene and polytetrafluoroethylene composites. Two research methods used free space measurement set up with frequency extenders (Kang & Kim, 2019; Vohra & El-Shenawee, 2021). Different types of horn antennas were used. One of it was corrugated horn antenna for W-band (Kang & Kim, 2019) while conical lens horn antennas were utilized too for free space material measurement system (Gonçalves et al., 2018; Vohra & El-Shenawee, 2021). Besides, (Hajisaeid et al., 2018; Malik et al., 2019) proposed a pair of horn antennas for the free space material measurement system.

Table 2.2 Free space material measurement systems

Ref	Free space method setup	Frequency (GHz)	Samples
<p>Kang & Kim, 2019</p>		<p>75 -110</p>	<p>-Air -Plastic plate</p>
<p>Vohra et al., 2020</p>		<p>20-25, 75-110</p>	<p>-radar absorbing materials</p>
<p>Gonçalves et al., 2018</p>		<p>1-6</p>	<p>-Polymethylmethacrylate (PMMA) -Polytetrafluorethylene (PTFE)</p>
<p>Hajisaacid et al., 2018</p>		<p>3-18</p>	<p>- polyimide film (Kapton), -liquid crystalline polymer sheet (LCP) -ceramic-filled polytetrafluoroethylene composites (RO3035) -polypropylene</p>

<p>Malik et al., 2019</p>		<p>26-32</p>	<p>- Polylactic Acid (PLA)</p>
--------------------------------------	---	---------------------	---------------------------------------

2.5 Characterization of dielectric materials

This section provides a comprehensive overview of how dielectric materials are characterized, along with recent advancements in assessing their properties through various measurement techniques. Transmission line measurements offer the advantage of determining both permeability and permittivity, but they are limited by air gap effects. Coaxial probe methods eliminate the need for sample machining but can be influenced by air gaps. Resonant cavity techniques excel in measuring very small materials under test but are restricted to a narrow frequency band. Free-space measurements are advantageous for high-frequency and non-destructive testing, yet suffer from multiple reflections between the sample and antenna, which can affect accuracy. Table 2.3 summarizes the advantages and disadvantages of different measurement techniques.

Table 2.3 Measurement Techniques Advantages and Disadvantages (Sivakumar et al., 2023)

Measurement techniques	Advantages	Disadvantages
Transmission Line	Able to determine both the permeability and permittivity	Has the limitation of the air gap effects
Coaxial Probe	No machining of sample is needed	Influenced by air gaps
Resonant cavity	Able to measure very small MUT	Restricted to narrow band of frequencies only
Free-space	Able to use for high frequency measurement, permits non-destructive measurement	Multiple reflections between the sample and the antenna

The work in (García-Pérez et al., 2017; Liu et al., 2020) demonstrated a quasi-optical concept using dielectric lenses for free-space measurement system. The various measured samples with different thicknesses indicated dielectric constant, ϵ_r' which closely resembles their nominal values. However, the loss tangents, $\tan \delta$ for the same material with different thicknesses are rather different, as tabulated in Table 2.4. This is especially evident in low-loss materials such as styrofoam and Teflon. For thinner (250 μm) Teflon samples, there exists a larger difference in nominal and measured $\tan \delta$. Moreover, thinner samples which are less than 500 μm are more difficult to measure accurately. Nonetheless, the $\tan \delta$ for Hostafon and Kapton are similar with those provided by the manufacturer.